



1 **Mineral nutrients in Saharan dust and their potential impact on Amazon**
2 **rainforest ecology**

3

4 Joana A. Rizzolo¹, Cybelli G.G. Barbosa¹, Guilherme C. Borillo¹, Ana F.L. Godoi¹,
5 Rodrigo A.F. Souza², Rita V. Andreoli², Antonio O. Manzi³, Marta O. Sá³, Eliane G.
6 Alves³, Christopher Pöhlker⁴, Isabella H. Angelis⁴, Florian Ditas⁴, Jorge Saturno⁴, Dan-
7 iel Moran-Zuloaga⁴, Luciana V. Rizzo⁵, Nilton E. Rosário⁵, Theotonio Pauliquevis⁵,
8 Carlos I. Yamamoto⁶, Meinrat O. Andreae⁴, Philip E. Taylor^{7*}, and Ricardo H.M.
9 Godoi^{1**}

10

11 *Corresponding Authors: School of Life and Environmental Sciences, Deakin Uni-
12 versity, Australia. e-mail address: philip.taylor@deakin.edu.au (P.E.Taylor*); Envi-
13 ronmental Engineering Department, Federal University of Parana, Brazil. e-mail ad-
14 dress: rhmgodoi@ufpr.br (R.H.M. Godoi**).

15

16 ¹ Environmental Engineering Department, Federal University of Parana, Curitiba, PR,
17 Brazil.

18 ² State University of Amazonas - UEA, Meteorology Department, Manaus, AM, Brazil.

19 ³ Instituto Nacional de Pesquisas da Amazônia, Programa de Grande Escala Biosfera
20 Atmosfera na Amazônia, Manaus, Brasil.

21 ⁴ Max Planck Institute for Chemistry, Biogeochemistry Department, Mainz, Germany.

22 ⁵ Universidade Federal de São Paulo, Instituto de Ciências Ambientais, Químicas e
23 Farmacêuticas, Diadema, Brasil.

24 ⁶ Chemical Engineering Department, Federal University of Parana, Curitiba, PR, Brazil.



25 ⁷Deakin University, CCMB and CMMR, School of Life and Environmental Sciences,
26 Geelong, Vic, Australia.

27

28 **Abstract**

29 The intercontinental transport of aerosols from the Sahara is likely to play a significant
30 role in nutrient cycles in the Amazon rainforest, since it carries many types of minerals
31 to these otherwise low-fertility lands. Iron is one of the micronutrients essential for
32 plant growth, and the Amazon rainforest is iron-limited. The main aim of this study was
33 to assess the input and potential impact of iron bioavailability from Saharan dust, name-
34 ly, the soluble fraction Fe(II)/Fe(III). Seven other soluble elements that are also essen-
35 tial for plants were measured. Dust particles entrained in the air were collected and ana-
36 lyzed, but not dust deposited in rainfall as atmospheric washout. The sampling cam-
37 paign was carried out at the ATTO site (Amazon Tall Tower Observatory), from March
38 to April 2015, and samplers were placed both above and below the canopy. Mineral
39 dust aerosol at ATTO showed peak concentrations for Fe(III) (47.6 ng m⁻³), Fe(II) (16.2
40 ng m⁻³), Na (470 ng m⁻³), Ca (194 ng m⁻³), K (64.7 ng m⁻³), and Mg (88.8 ng m⁻³) during
41 the presence of dust transported from the Sahara, as determined by remote ground-based
42 and satellite sensing data and backward trajectories. Atmospheric transport of weathered
43 Saharan dust, followed by surface deposition, results in substantial iron bioavailability
44 across the rainforest canopy. The seasonal deposition of dust rich in soluble iron and
45 other minerals is likely to affect both bacteria and fungi within the topsoil and on cano-
46 py surfaces, and especially benefit highly bioabsorbent epiphytes, such as lichens. In
47 this scenario, Saharan dust can provide essential macronutrients and micronutrients to
48 plant roots, and also directly to plant leaves. The influence on the ecology of the forest



49 canopy and topsoil would likely be different from that of nutrients from the weathered
50 Amazon bedrock, which provides the main source of soluble mineral nutrients.

51 **Key words:** Amazon forest, Sahara dust, mineral nutrients, bioavailable, soluble iron,
52 outbreak event, dust transport

53 **1 Introduction**

54 The Sahara is the largest source of desert dust to the atmosphere (Ginoux et al.,
55 2012). Studies are beginning to reveal the extent of the Saharan dust influence on nutri-
56 ent dynamics and biogeochemical cycling in both oceanic and terrestrial ecosystems in
57 North Africa and far beyond, due to frequent long-range transport across the Atlantic
58 Ocean, the Mediterranean Sea and the Red Sea, and on to the Americas, Europe and the
59 Middle East (Goudie and Middleton, 2001; Hoornaert et al., 2003, Yu et al., 2015; Sal-
60 vador et al., 2016).

61 Saharan dust affects climate and atmospheric chemistry at both regional and
62 global scales. Large scale and mesoscale atmospheric circulation have a key role to play
63 in the emission and transport of mineral aerosols. Research is ongoing into the effects of
64 year to year and decade to decade variability of loadings and transport of dust in the
65 atmosphere (Washington and Todd, 2005).

66 The Amazon Basin, which contains the world's largest rainforest (Garstang et
67 al., 1988; Aragão, 2012; Doughty et al., 2015) receives annually about 28 million tons
68 of African dust each year (Yu et al., 2015). There have been suggestions that Saharan
69 dust transport across the Atlantic may act as a valuable fertilizer of the Amazon rainfor-
70 est, providing fundamental nutrients (Swap et al., 1992; Koren et al., 2006; Ben-Ami et
71 al., 2010; Abouchami et al., 2013). However, little is known about the bioavailability of
72 these nutrients and their potential affect on rainforest ecology. It is, therefore, important



73 to understand the source types, source strengths, and the physical and chemical proper-
74 ties of mineral dust aerosol particles over the Amazon Basin (Guyon et al., 2004).

75 Plants require many nutrients for healthy development (Marschner, 2012). Iron
76 (Fe) is an essential micronutrient for plant growth (Morrissey and Guerinot, 2009) and it
77 is a key element in several important functions and physiological processes. It partici-
78 pates in chlorophyll function and is required for enzymes critical for photosynthesis,
79 such as catalase, peroxidase, nitrogenase, and nitrate reductase (Hochmuth, 2011). Plant
80 bio-functions, such as photosynthesis, respiration and hormonal balance, also require
81 Fe, along with other elements (Pérez-Sanz et al., 1995).

82 Under natural soil conditions, Fe(III) occurs bound to minerals, such as hema-
83 tite, that are not soluble in water (Isaac, 1997; Zhu, 1997), and Fe dissolution is depend-
84 ent on the water's ligand capacity as well as on than the type or quantity of dust deposit-
85 ed on the surface (Mendez, 2010).

86 Two distinct pathways of Fe uptake have been identified in plant roots. Pathway
87 I, present mainly in dicot plants, reduces Fe(III) to Fe(II) by acidification of the rhizo-
88 sphere. After this reduction, Fe(II) is transported into cells. In pathway II, compounds
89 with high affinity for iron are secreted into the rhizosphere, where they react with
90 Fe(III) and form a chelate complex. This complex is moved into cells by specific trans-
91 porters (Hell and Stephan, 2003; Morrissey and Guerinot, 2009). In the forest, microor-
92 ganisms, such as fungi and bacteria, play a role in nutrient cycling, and often employ
93 multiple distinct iron-uptake systems simultaneously (Philpott, 2006).

94 Furthermore, Fe-rich dust particles can be transported over long distances and
95 have considerable time and surface area to take up acids (Shi et al., 2011). An increased
96 proportion of soluble iron has recently been reported in high altitude Saharan dust com-
97 pared with ground-based samples (Ravelo-Perez et al., 2016). Thus, particle size, solu-



98 bility, and bioaccessibility of iron oxides in dust will determine the ultimate influence of
99 these materials on environmental and biological processes (Reynolds, 2014).

100 Besides iron uptake, other elements are also essential for plants. Magnesium and
101 Cu are required for photosynthesis and protein synthesis. Calcium is essential for cell
102 wall and membrane stabilization, osmoregulation, and as a secondary messenger allow-
103 ing plants to regulate developmental processes in response to environmental stimuli
104 (Gruzak, 2001). Zinc is directly involved in the catalytic function of many enzymes, and
105 with regulatory and structural functions (Broadley et al., 2007). Potassium regulates
106 osmotic pressures, stomata movement, cell elongation, cytoplasm pH stabilization, en-
107 zymatic activation, protein synthesis, photosynthesis, and transport of sugars in the
108 phloem (Kerbaui, 2012).

109 Atmospheric mineral dust contributes thousands of tons of minerals to tropical
110 rain forests (Okin et al., 2004; Bristow et al., 2010) and likely contributes to plant nutri-
111 tion, especially compensating for the poor soils with low inherent fertility (Worobiec et
112 al., 2007). Amazon lowland rainforest soils are shallow and have almost no soluble
113 minerals; added to this, heavy rains readily leach soluble nutrients from the ground that
114 are added from litter decomposition and weathered rocks (Koren et al., 2006).

115 Saharan desert aerosol can compensate for P leaching from the poor soils of the
116 Amazon (Gross et al., 2015). Intercontinental transport of dust is likely to be of great
117 importance to the forest, as it might help to maintain or possibly influence an ecosystem
118 that has roles in global climate regulation, in addition to maintaining regular rainfall and
119 storing vast amounts of carbon (Karanasiou et al., 2012). A number of studies have stat-
120 ed that Saharan dust contributes as a fertilizer to the forest (Swap et al., 1992; Koren,
121 2006; Bristow et al., 2010; Martin, 2010; Abouchami et. al, 2013; Yu et al., 2015). Oth-



122 er than for P, the amount of this dust that is available to plants as soluble micronutrients
123 and macronutrients is unknown, as is the potential influence on forest ecology.

124 Considering that iron is absorbed by plants only as soluble Fe(II)/Fe(III), it is es-
125 sential to quantify the intake of this mineral from long-range transported African dust,
126 and evaluate its potential utilization and effect on the Amazon rainforest as an essential
127 micronutrient. This research aims to assess the bioavailability of iron, and other ele-
128 ments in the particulate matter in the Amazon atmosphere transported within African
129 dust. This is then used to assess the likely effect on rainforest ecology.

130

131 **2 Methods**

132 **2.1 Dust sampling**

133 Sampling was performed on a 80 m walk-up tower at the Amazon Tall Tower
134 Observatory (ATTO) site (Andreae et al., 2015), from 19 March to 25 April 2015,
135 which is within the typical period that dust transport to the Amazon Basin has been ob-
136 served (Swap et al., 1992; Prospero et al., 2014; Yu et al., 2015). Aerosols were sam-
137 pled above the canopy at 60 m height and below the canopy at 5 m height, without size
138 cut-off, and transported in a laminar flow through a 2.5 cm diameter stainless steel tube
139 into an air-conditioned container. The sample humidity at 60 m height was kept below
140 40% using a silica dryer. The sample humidity at 5 m height was kept dry with a silica
141 gel diffusion dryer installed on the inlet line. Atmospheric particles were collected on
142 Nuclepore® polycarbonate filters at a flow rate of 10 l min⁻¹.

143 The aerosol sampling was performed using the inlet below the canopy at 5 m
144 height for the first 11 days, and the inlet at 60 m height for the other 26 days. The sam-
145 ples were collected over 24 or 48 h periods, consecutively, in order to accumulate suffi-
146 cient mass to be detected by ion chromatography-UV-VIS. After sampling, the filters



147 were immediately stored in flasks containing nitric acid solution (HNO_3 Suprapur) pH
148 2.0-2.5, in order to interrupt the transition process between the two iron oxidative states
149 (Fe(II) and Fe(III)) and to stabilize the iron concentrations, according to the methodolo-
150 gy adapted from Siefert (1998), Bruno et al. (2000), and US-EPA Method 3052 (EPA,
151 1996).

152

153 **2.2 Particle physical properties**

154 Aerosol particle physical properties were determined at ATTO during the entire
155 campaign at 60 m height. Mass concentration and particle size distribution were meas-
156 ured by an Optical Particle Sizer (OPS, TSI model 3330; size range: 0.3–10 μm), sam-
157 pling every 5 min (Andreae et al., 2015). Equivalent black carbon concentrations (BC_e)
158 were obtained by a MAAP (Multi Angle Absorption Photometer), and the spectral de-
159 pendency of particle absorption coefficients was determined using a 7-wavelength Ae-
160 thalometer (Model AE33), both with 1 min resolution. Particle scattering coefficients
161 were obtained at three wavelengths using an Integrating Nephelometer (Ecotech, model
162 Aurora 3000). Details of the instrumentation setup are given by Andreae et al. (2015).

163

164 **2.3 Determination of mineral aerosol**

165 Soluble species were determined by ion chromatography (Dionex, ICS-5000) us-
166 ing conductivity detection for cations and UV-VIS for soluble transition metals. For
167 cation separation, a capillary column CS12A was used, and for transition metals, a
168 CS5A column (calibrated to quantify traces of Fe(II) and Fe(III)). Each analysis oc-
169 curred in triplicate and all measurements were performed from a standard curve injected
170 under the same conditions as the samples, using Chromeleon® software for processing
171 the generated chromatograms.



172

173 **2.4 Modeling, remote sensing and meteorological data**

174 Air mass backward trajectories were calculated using the Hybrid Single Particle
175 Lagrangian Integrated Trajectory (HYSPLIT) Model from the NOAA Air Resource
176 Laboratory, USA, (National Oceanic and Atmospheric Administration), indicating the
177 airflow toward the ATTO site (Draxler and Rolph, 2015). Thus, dust source areas were
178 inferred by tracking individual dust plumes back to their place of origin (Schepanski et
179 al., 2012) as well as determining transport paths. Trajectories were calculated at three
180 different heights within the atmospheric boundary layer (50, 500, and 1000 m) up to
181 240 h previous. Every 24 h from 19 March to 25 April 2015, a trajectory was calculated
182 with a finishing point at the center of the ATTO site (S 2° 08.752' W 59° 00.335'), at 19
183 h UTC.

184 To analyze Saharan dust outbreak events and transport toward ATTO during the
185 campaign, ground-based and satellite remote sensing products and *in situ* measurements
186 of aerosol particle optical properties were integrated with the atmospheric large-scale
187 wind field. The wind field product was taken from the Modern-ERa Retrospective
188 Analysis (MERRA), a reanalysis data based on the Goddard Earth Observing System
189 Data Assimilation System Version 5 (GEOS-5, Rienecker et al., 2011). Ground-based
190 and satellite remote-sensing aerosol optical properties, namely Aerosol Optical Depth
191 (AOD), were obtained, respectively, from aerosol products of the AErosol RObotic
192 NETwork (AERONET, Holben et al., 1998) and of the Moderate-Resolution Imaging
193 Spectroradiometer (MODIS) aboard the Terra satellite (Remer et al., 2005). Particle
194 optical properties were continuously monitored *in situ* at the ATTO site in 2015 at a
195 height of 55 m. Particle scattering coefficients were measured at three wavelengths us-
196 ing an integrating nephelometer (Ecotech Aurora 3000). Absorption coefficients were



197 measured at 637 nm using a Multi-Angle Aerosol Photometer (MAAP). Particle single
 198 scattering albedo was calculated based on measured absorption and scattering retrieved
 199 by interpolation at 637 nm. All measurements were taken under dry conditions
 200 (RH<50%).

201 Micrometeorological data were obtained by sensors installed on the micromete-
 202 orological tower at the ATTO site, at 80 m (Andreae et al., 2015). Daily values were
 203 calculated for vertical wind speed median (W), accumulated precipitation (PRP), and
 204 average air temperature (Tair).

205 Table 1 shows the sampling frequencies, micrometeorological measurements,
 206 sensors (manufacturers), and sensor heights. For the treatment of high frequency data
 207 (10Hz), computational routines were used. First, the sonic raw data was reduced to 1-
 208 min medians. Subsequently, daily values were calculated.

209

210 Table 1. List of instruments installed on the walk-up tower (adapted from Andreae et
 211 al., 2015).

Sampling frequency	Measurement	Instrument used	Height/Depth (m)	Unit
0.1 s	u, v,w (wind compo- nents)	3D ultrasonic anemometer (Windmas- ter, Gill Instruments Ltd.)	81.65; 46.0; 36.0	m/s
60 s	Rainfall	Rain gauge (TB4, Hydrological Ser- vices Pty. Ltd.)	81.0	mm
	Air temperature probe	Thermohygrometer (HMP45C, Vaisala, CS215, Rotronic Measure- ment Solutions)	81.65; 40.0; 36.0	°C

212

213

214 2.5 Spore samples

215 A Sporewatch spore sampler (Burkard Scientific Pty Ltd, UK) was operated at
 216 80 m height for 24 h on 16 separate days between 28 March and 23 April. Particles



217 larger than 2 μm diameter were impacted onto an adhesive-coated tape attached to a
218 drum within the sampler. This tape was removed, mounted onto a microscope slide and
219 examined with an Olympus BX60 light microscope with brightfield optics. Line scans
220 were performed to identify fungi, and counts were averaged over 24 h and expressed per
221 cubic meter of air sampled. All aerosol concentrations are given with respect to air vol-
222 umes at ambient temperature and pressure.

223 **3 Results and discussion**

224 The sampling campaign was performed during a typical period for the occur-
225 rence of dust transport events in the Amazon forest. Sampling covered a total of 38 days
226 (19 March– 25 April 2015) and 26 samples of particulate matter were collected.

227

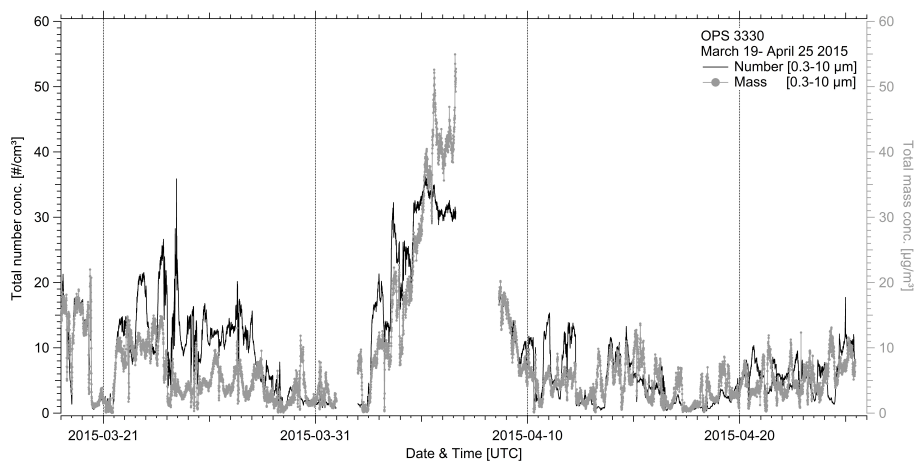
228 **3.1 Characterization of particle physical properties**

229 The mass concentration of particles over the Amazon Basin in the wet season is
230 typically around $10 \mu\text{g m}^{-3}$ in locations that are influenced by biomass burning emis-
231 sions. In the central Amazon, where the influence of biomass burning is less, the mass
232 concentration is even lower. However, elevated concentrations may occur due to Afri-
233 can dust events that reach the Amazon forest (Martin et al., 2010). The highest hourly
234 aerosol concentration recorded during our entire campaign was around $55 \mu\text{g m}^{-3}$ at the
235 ATTO site (5 April), with a daily average of $23 \mu\text{g m}^{-3}$ (Figure 1), and often concentra-
236 tions were well below $10 \mu\text{g m}^{-3}$. Previous studies conducted by Worobiec et al. (2007)
237 at a nearby forest site in Balbina, Amazonia, had also detected an abundance of dust
238 particles during the same season (23 - 29 March 1998). Artaxo et al. (2013) observed,
239 only trace levels of P, K, and Zn during the wet season in the central Amazon region.
240 These were thought to have a biogenic source.

241



242



243

244 Figure 1. Number concentration (solid lines) and mass concentration (dashed lines) time
245 series from the OPS instrument (size range: 0.3-10 μm).

246

247 For comparison, during Saharan dust events in the Cape Verde archipelago, par-
248 ticulate matter concentration often exceeds $100 \mu\text{g m}^{-3}$; a relatively high concentration
249 when compared to the average aerosol background level of $10\text{-}50 \mu\text{g m}^{-3}$ (Gross et al.,
250 2015). Obviously, the enhancement in concentrations induced by the plume is highest
251 near the source, so a larger mass of dust is deposited over the Sahara and the adjacent
252 Atlantic than over the Amazon rainforest. Notably, the concentrations at ATTO were
253 still very high in view of the large distance from Africa.

254 The highest concentrations of black carbon equivalent (BC_e) measured online
255 during this intensive campaign were $0.45 \mu\text{g m}^{-3}$ (3 April) and $0.37 \mu\text{g m}^{-3}$ (5 April).
256 This coincided with the highest mass concentrations of particulate matter. The BC_e con-
257 centrations were retrieved from light absorption measurements. The particle types that
258 mostly contribute to light absorption are: combustion generated BC, mineral dust, and
259 biogenic particles (Moosmüller et al., 2009; Guyon et al., 2004). Therefore, part of the



260 observed BC could be mineral dust. We further characterized the relative contributions
261 to BC_e by considering the Absorption Angstrom Exponents (AAE), which reflect the
262 spectral variability of absorption. Bulk BC particles are expected to have an AAE ≤ 1
263 due to increased absorption efficiency at shorter wavelengths (<400 nm). The observed
264 variability of AAE is further discussed in section 3.3. During the 2008 wet season in the
265 central Amazon, at a site near Manaus, BC_e concentrations fluctuated between 0.10 and
266 $0.15 \mu\text{g m}^{-3}$ (Martin et al., 2010). Episodic input of Saharan dust and biomass smoke
267 transported over long distances from Africa explains the presence of BC_e detected at
268 ATTO (Andreae et al., 2015).

269

270 **3.2 Determination of Mineral Aerosol**

271 The dominant elements in the soluble fraction of the dust samples were Fe(III),
272 Zn, Na, K, and Mg (Table 2). The blank fields in the Table correspond to values below
273 the detection limits, which were calculated according to Method 300.1 USEPA (1997).
274 The expanded uncertainty (ng m^{-3}) was calculated for 95% confidence level, according
275 to BIPM/GUM (2008).

276



277 Table 2. Mineral aerosol characterization of 26 samples collected during the Saharan
 278 dust event that arrived in the Amazon forest during 2015.

Sampled period (Month/day)	Fe(III) (ng m ⁻³)	Fe(II) (ng m ⁻³)	Cu (ng m ⁻³)	NH ₄ (ng m ⁻³)	Zn (ng m ⁻³)	Na (ng m ⁻³)	Ca (ng m ⁻³)	K (ng m ⁻³)	Mg (ng m ⁻³)
3-19	15±0.7	-	-	147±4	105±8	95±7	92±13	54±12	13±2
3-19	11±0.8	-	-	-	14±7	41±6	-	40±8	9.0±1.0
3-20	5.6±0.1	-	-	163±1.7	6.5±3.7	-	-	-	-
3-21	5.8±0.1	-	-	-	3.5±1.8	84±6	40±3	26±3	13±1
3-23	7.1±0.1	-	-	56±2	6.4±3	73±3	-	40±4	10.1±0.5
3-24	4.8±0.1	-	-	33±1	4.2±1.9	25±2	-	29±2	3.0±0.3
3-25	1.8±0.1	-	-	-	2.0±0.9	44±3	-	32±2	6.0±0.6
3-27	2.0±0.1	-	-	-	3.4±1.6	12±1	-	22±2	1.7±0.2
3-28	1.9±0.2	-	0.89±0.87	9.7±1.8	5.0±2.2	18±2	5.9±2.5	25±3	2.6±0.3
3-30	4.1±0.1	-	-	5.2±1.3	5.8±3.8	10±3	-	-	1.2±0.5
3-31	4.1±0.1	-	2.7±0.8	-	4.7±1.9	17±2	-	8.0±5.4	1.7±1.1
4-02	8.5±0.1	-	2.5±1.5	-	8.3±3.7	135±3	12±6	32±4	16±1
4-03	33±0.1	-	-	-	4.6±1.8	441±4	126±4	65±2	67±1
4-05	48±0.1	16±3	-	-	8.4±3.6	470±4	194±4	64±4	89±1
4-06	33±0.1	12±2	0.85±0.75	-	4.3±1.9	220±22	128±8	44±4	49±3
4-08	14±0.2	3.3±3.1	-	16±1	8.9±3.7	148±3	29±4	26±4	244±2
4-09	19±1	1.6±1.6	-	6.6±0.8	5.3±1.9	57±2	29±2	15±2	8.6±0.3
4-11	5.5±0.1	-	-	68±1	9.7±3.7	84±3	-	18±4	8.8±0.5
4-12	5.7±0.2	-	6.4±0.8	-	5.7±1.9	38±2	5.0±1.9	9.6±2.2	5.5±0.2
4-14	6.7±0.2	-	-	20.4±1.19	10.2±3.68	24±3	-	9.4±4.3	3.2±0.5
4-15	12±0.1	-	88±1	98.5±5.45	-	15±2	-	7.4±2.05	10±1
4-17	7.4±0.2	-	9±1	-	10.2±3.9	24±3	-	8.2±4.5	3.7±0.5
4-18	1.1±0.1	-	2.6±0.8	-	4.8±1.7	19±2	3.5±1.7	9.7±2.2	2.7±0.2
4-20	1.2±0.2	-	-	370±1	9.5±3.5	29±3	8.6±3.5	20±4	5±0.6
4-21	2.9±0.2	-	13±0.7	55±1	2.1±1.7	14±2	-	-	4.30±0.2
4-23	2.4±0.1	-	1.0±0.8	-	2.2±1.9	28±2	-	5.4±2.2	3.1±0.3



279 During the wet season in the central Amazon Basin, Artaxo et al. (2002), Martin
280 et al. (2010), and Arana and Artaxo (2014), found similar values of K, Fe, Cu and Zn to
281 those found in our campaign. K, Cu, and Zn are generally considered to be tracer ele-
282 ments of biogenic emissions from the rainforest, although they also have other sources.
283 Potassium in submicron aerosols also has a major source from vegetation fires and is
284 frequently used as a tracer for biomass burning aerosols (Andreae et al., 1983; Martin et
285 al., 2010). Zhang et al. (2015) studied aerosols from a Chinese tropical rainforest, and
286 reported that the high abundance of K in fine particles was likely a result of long-range
287 transport from biomass burning.

288 Iron, Ti and Al are mainly soil dust related elements (Artaxo et al., 1990; Artaxo
289 et al., 1994), and are typically present at the highest concentrations during the early wet-
290 to-dry season transition (February to May), as has been shown in previous studies
291 (Pauliquevis et al., 2012; Andreae et al., 2015). This is mainly driven by large-scale
292 atmospheric circulation patterns that favor the transport of dust plumes in a trans-
293 Atlantic airflow from the Sahara and Sahel regions toward the Amazon basin (Artaxo et
294 al., 1990; Formenti et al., 2001; Graham et al., 2003; Martin et al., 2010; Baars et al.,
295 2011; Ben-Ami et al., 2012).

296 During the wet season, the biogenic aerosol over Amazonia is overprinted peri-
297 odically by episodes of intense transatlantic transport, which bring Atlantic marine aer-
298 osols in addition to dust and biomass burning emissions (Bristow et al., 2010; Andreae
299 et al., 2015). For example, Zhu et al. (1997) studied North African dust entrained in the
300 trade winds over Barbados (Caribbean) in September, and measured Na concentrations
301 of 2.4 to 6.5 $\mu\text{g m}^{-3}$. Barbados is in a region that receives large amounts of Na enriched
302 marine aerosols due its localization. While these concentrations are higher than those
303 recorded in the present study at ATTO (220 to 470 ng m^{-3}), the co-occurrence of elevat-

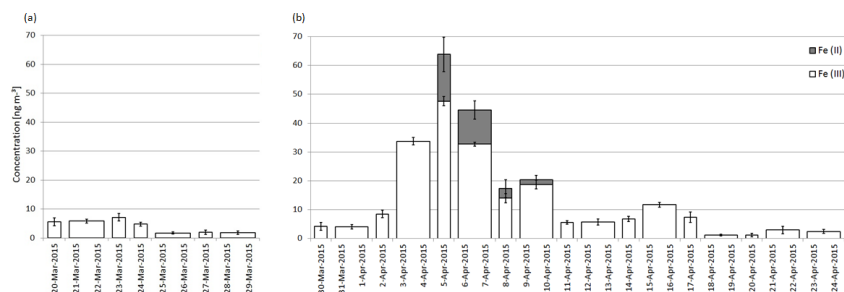


304 ed concentrations of Na and the mineral dust elements, Al, Fe, and Ca, is evidence for
305 the marine origin of Na in the central Amazon (Talbot et al., 1990).

306 Artaxo et al. (1990) studied aerosols from the Amazon Basin and noted that the
307 concentration of total Fe in the fine mode ($<2.5 \mu\text{m}$) of soil dust were more than 10
308 times larger in the wet season than in the dry season (101 ng m^{-3} during daytime, 60 ng
309 m^{-3} during the night and 6.5 ng m^{-3} in the dry season). Pauliquevis et al. (2012) observed
310 increases in the concentration of total Fe with values reaching 60 ng m^{-3} in the fine
311 mode mostly during February to April in the Amazon Basin, with a semester average of
312 36 ng m^{-3} . They attributed this to episodes of Saharan dust transport.

313 In contrast to the high bulk dust concentrations at Barbados, the Fe(II) concen-
314 trations recorded at ATTO during our sampling campaign (1.6 to $16 \mu\text{g m}^{-3}$) were sig-
315 nificantly higher than the Fe(II) concentrations of 0.63 to 8.2 ng m^{-3} measured in miner-
316 al dust particles collected from the marine atmospheric boundary layer at Barbados (Zhu
317 et al., 1997). They showed that only a small fraction of the total iron in aerosol particles
318 was present as Fe(II).

319 For soluble Fe(III), we found concentrations in the range of 1.10 to 47.6 ng m^{-3}
320 (Figure 2), with the highest concentrations occurring three days in a row (33.7 , 47.6 and
321 32.7 ng m^{-3}). This soluble Fe(III) is carried in dust particles that are mainly deposited
322 onto canopy surfaces by dry sedimentation. Our soluble Fe(III) concentrations were
323 significantly higher than those reported by Andreae et al. (2015) from earlier measure-
324 ments at the same site. They had measured only 1.8 ng m^{-3} of soluble Fe(III) in 120 ng
325 m^{-3} of total Fe and concluded that the aerosol transport of Fe is not likely to have a sig-
326 nificant effect on the ecosystem at ATTO.



327

328 Figure 2. Soluble Fe(III) and Fe(II) concentrations in total particulate matter collected
329 during the wet season, (a) sampled at 5 m height (20 March to 29 March 2015) and (b)
330 at 60 m height (30 March to 24 April 2015). The width of bars corresponds to the sam-
331 pling period: 24 or 48 h.

332

333 Desert dust plumes contain iron mainly in the Fe(III) oxidation state, whereas in
334 industrial effluents Fe is mostly in the Fe(II) oxidation state (Reynolds et al., 2014).
335 These same authors collected dust from the Sydney area (Australia) and strongly sug-
336 gested that the addition of Fe(II)-bearing minerals was associated with industrial, urban,
337 and transportation sources entrained in dust plumes that originally lacked these miner-
338 als.

339 Bristow et al. (2010) analyzed aerosol samples collected from the Bodélé De-
340 pression, Chad, and suggested that the amounts of Fe in some samples likely indicate
341 the presence of ferromagnesian minerals and also reflect the presence of Fe oxides such
342 as goethite and hematite, or Fe sulfate salts that have been detected in Saharan dust.

343 Abouchami et al. (2013), studying the geochemical characteristics of the Bodélé
344 Depression dust source and the relation with transatlantic dust transport to the Amazon
345 Basin, found lower Na, K, Fe, and Ca concentrations in Amazon Basin soil samples
346 than in the Bodélé samples, suggesting that this difference is a reflection of remobiliza-



347 tion and loss of these elements by chemical weathering under the hot, wet climate con-
348 ditions in the Amazon Basin.

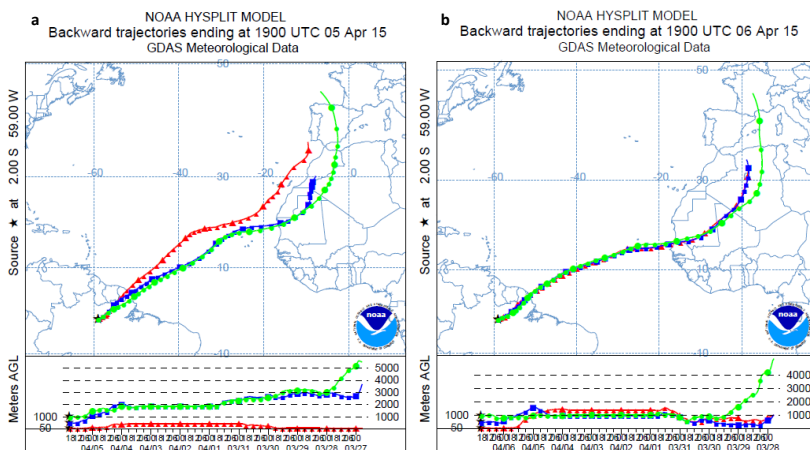
349

350 3.3 Modeling, Remote Sensing and Meteorological Data

351 The largest deposition of iron occurs downwind of the main deserts of the world
352 - North Africa and the Middle East (Mahowald et al., 2009). Figure 3 (a and b) shows
353 the backwards trajectories coming not from North Africa nor the Middle East, but in-
354 stead from the Saharan desert (Formenti et al., 2001; Washington and Todd, 2005; Bris-
355 tow et al., 2010; Creamean et al., 2013). Koren et al. (2006) estimated that between No-
356 vember and March, the Bodélé Depression is responsible for most of the dust that is
357 deposited annually on the Amazon.

358 Using backward trajectories data (HYSPLIT model), it is possible to observe a
359 connection between the Sahara and the Amazon. Between 3 and 6 April, the highest
360 concentrations of Fe(III), Fe(II), Na, Ca, K and Mg in mineral dust samples were ob-
361 served. According to Figure 3, the air masses arriving in the Amazon during that period
362 came from the Saharan region.

363



364



365 Figure 3. Backward trajectories of air parcels at 50, 500, and 1000 m above the Amazon
366 for 240 h during the sampling periods in which the greatest concentrations of dust from
367 the Sahara arrived at ATTO.

368

369 High mass concentrations around 3-8 April 2015 coincided with the arrival of
370 African dust in the Amazon Basin, according to OPS instruments and backward trajec-
371 tories, respectively, Figure 1 and 3. Periodically in the wet season, long-range transport
372 of sea spray, Saharan dust, and/or smoke from African biomass burning can deposit
373 across the Amazon Basin (Martin et al., 2010; Baars et al., 2011; Andreae et al., 2015).

374 As identified by the AERONET ground based sunphotometers located in Dakar
375 and in Ilorin, during the campaign period three major Saharan dust outbreaks occurred
376 and eventually combined with smoke (Figure 4.a). The first outbreak peaked on 22
377 March and had a stronger effect on AOD over Ilorin compared to Dakar. This feature
378 was corroborated by the MODIS mean AOD field from 20 to 25 March (Figure 5.a).
379 During this first event, the atmospheric circulation was not able to promote a significant
380 transport of the dust and smoke plume towards South America. The influence of Afri-
381 can particle advection on aerosol optical properties observed at ATTO was weak, but
382 still detectable. An increase in absorption and scattering coefficients was observed in
383 comparison to the clean periods (25 March to 2 April and 16-24 April), however, no
384 significant increase of AAE was observed during this event (Figure 4.b). A less active
385 dust outbreak from 25 to 30 March followed the first event, as shown by ground-based
386 and satellite data (Figure 4.a and 5.b).

387 A second dust outbreak event started at the beginning of April, according to the
388 AERONET retrievals, and its effects on the African sites extended until 9 April. The
389 satellite mean AOD field during this period (Figure 5.c) revealed a consistent pattern of

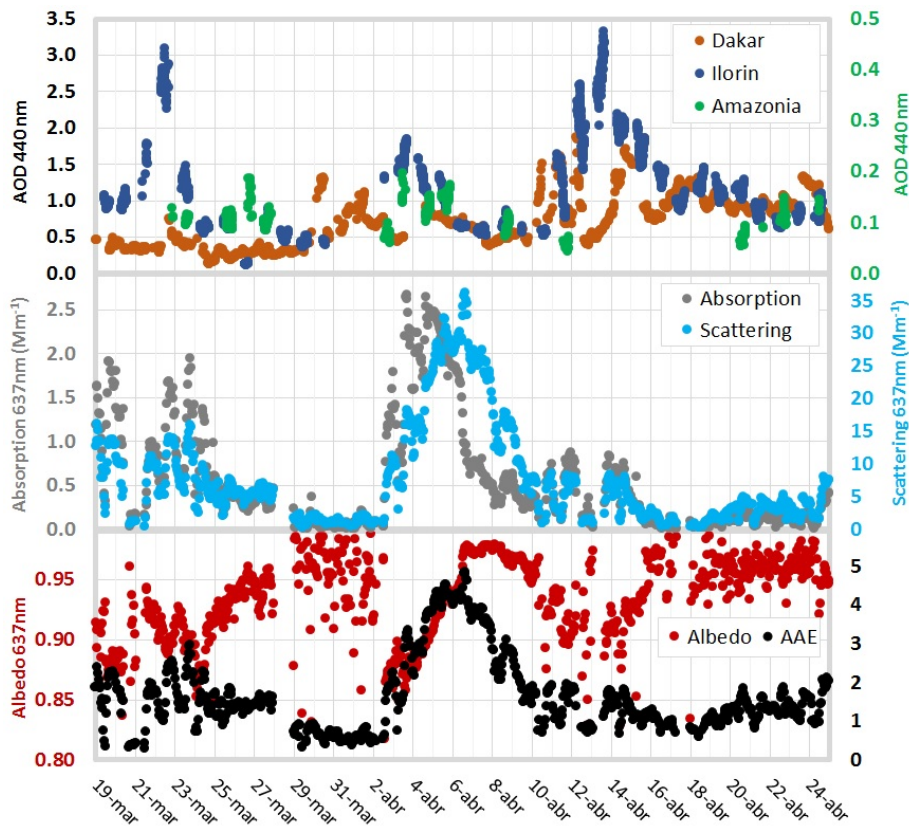


390 dust transport towards the northeast portion of the Amazon basin, with the wind flow in
391 the direction of ATTO coming from regions effectively influenced by the Saharan dust
392 plume. It is possible that smoke from biomass burning in the African sub-Sahel region
393 joined with dust aerosols transported to the Amazon, since the Ilorin region is affected
394 by biomass burning emissions in this season (Haywood et al., 2008). Fe(III) and Fe(II)
395 concentrations in particulate matter increased between 3 and 9 April (Figure 2), and this
396 correlated with an increase in particle absorption coefficients and a decrease in single
397 scattering albedo (Figure 4.b and 4.c). The AAE during this event reached values higher
398 than 5, and after 10 April returned to background levels. The increase in AAE is a
399 strong indication that dust and/or biomass smoke particles contributed to the observed
400 increases in absorption coefficients. The correlation between the concentration of crustal
401 elements in particulate matter and aerosol absorption coefficients during African
402 advection events has also been reported for another forest site in the Amazon (Rizzo et
403 al., 2013). The observed changes in particle optical properties can be explained by the
404 presence of Saharan dust particulate matter and biomass burning from the Sahel region.
405 Beside the appropriate transport direction, during the second event the wind circulation
406 speed was stronger than during the first event. This enhanced the Saharan dust advec-
407 tion toward ATTO and resulted in more substantial effects on particle chemical compo-
408 sition and optical properties at the site.

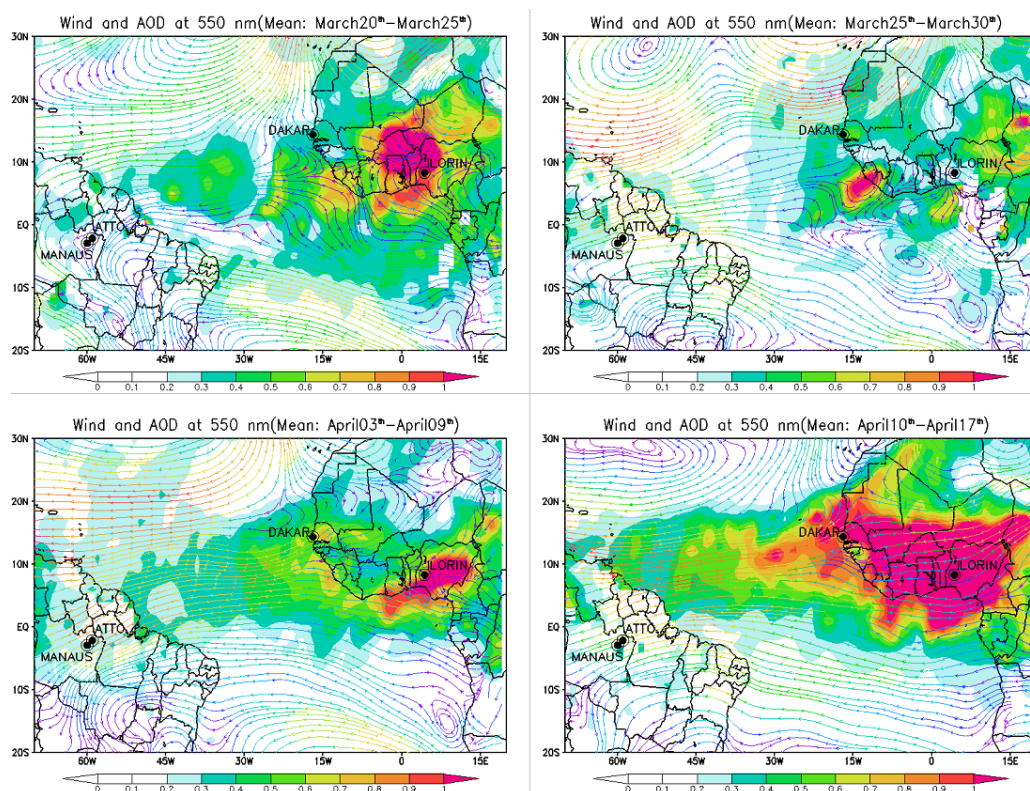
409 The third event that began around 10 April and lasted until 17 April, according
410 to the African AERONET sites (Figure 4.a), and was the largest dust outbreak event
411 that occurred during the campaign. This was corroborated by the significant increase
412 registered in the AERONET AOD and by the large values and spread of AOD retrieved
413 by MODIS (Figure 5.d). However, this massive dust transport toward the Atlantic basin
414 did not translate into significant changes in the properties of particles sampled at the



415 ATTO site. As happened in the first dust outbreak event, atmospheric wind circulation
416 prevented the transport of the dust plume in the direction of the ATTO site. At this time,
417 a strong zonal wind (eastward) from the African west coast carried the dust plume core
418 toward the extreme north portion of South America, away from ATTO. Meanwhile, the
419 site received an influx of air mass predominantly from an area southward of the plume.
420



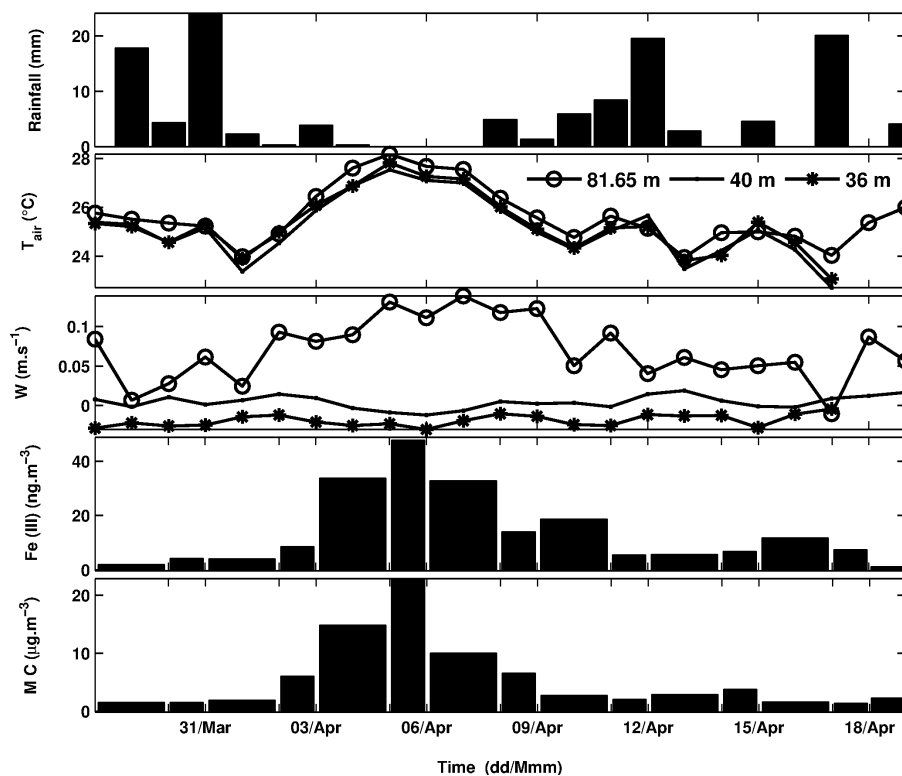
421
422 Figure 4. a) Instantaneous Aerosol Optical Depth (AOD) at 440 nm measured at three
423 AERONET sites: Dakar and Ilorin in Africa, and Embrapa/Manaus in Amazon. b) Par-
424 ticle absorption and scattering coefficients at 637 nm observed in situ at the ATTO site.
425 c) Particle single scattering albedo at 637 nm, and Absorption Angstrom Exponent
426 (AAE), retrieved from in situ observations of aerosol optical properties at ATTO.



427 Figure 5. Mean distribution of aerosol optical depth at 550 nm (AOD) and wind at 850
428 hPa for four distinct periods within the campaign at ATTO site, during the dominance
429 of: a) the first Saharan dust outbreak; b) a less active dust outbreak period; c) the second
430 Saharan dust outbreak; d) the third Saharan dust outbreak.

431 Figure 6 shows that during days without rainfall, the vertical wind speed, W ,
432 was highest above the canopy level (81.65 m), due to the canopy heating the air above
433 it. Without sunlight forcing, W values did not show significant difference at or below
434 the canopy (46 m and 36 m height, respectively). Levels below the canopy were, on
435 average, between a maximum of -0.0012 m/s and minimum of -0.03 m/s, and always
436 negative, although very close to zero.

437 At the highest level of W , being positive (ascending air), we also observed the
438 largest values for Fe(III) and MC.



439

440 Figure 6. Daily comparison of micrometeorological variables (T_{air} , PRP and W) with
441 measurements of Fe(III) and MC below the canopy.

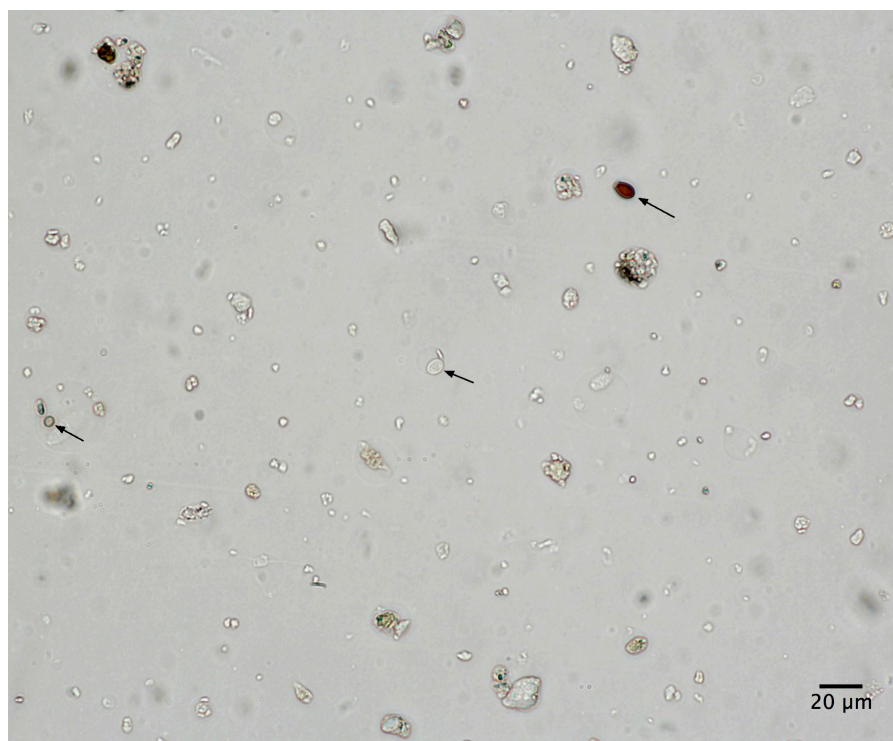
442

443 3.4 Spore sample

444 Sporewatch sample analysis showed that very few coarse particles ($> 2 \mu\text{m}$ di-
445 ameter) occurred in the atmosphere until 2 April. On 3 April at 13 LT, coarse particles
446 (2 to $10 \mu\text{m}$) peaked in number and were black, hyaline or variously colored and of ir-
447 regular shape. The amorphous particles were interspersed with a large diversity of small
448 fungal particles. Fungi that were identified included basidiospores, ascospores,
449 *Cladosporium*, *Ganoderma*, and uni- and bi-cellular hyaline conidia (Figure 7). All fun-
450 ghi detected had a diameter less than $12 \mu\text{m}$, similar to adjacent coarse dust particles. The
451 total fungal count was 1,587 spores per cubic meter of air, averaged over 24 h (2-3



452 April). High concentrations of fungi and other coarse particles persisted, peaking again
453 at approximately 16:30 LT on 5 April. From the afternoon of 6 April on, very few par-
454 ticles and only the occasional spore were observed.



455
456 Figure 7. Brightfield microscopy of particles collected in an air sampler at 80 m on 2
457 April 2015. The arrows point to three fungi: the one on the right is a basidiospore, at
458 center is a yeast-like conidia, and at left is a small fungal spore of unknown type.

459

460 As previously discussed, coarse particles observed between 2 and 6 April are
461 likely to be associated with the dust cloud arriving from Africa. The large diversity of
462 small fungal spores and conidia entrained in the dust collected at 80 m height are also
463 likely to be sourced to Africa. Smoke plumes are known to entrain fungi over long dis-
464 tances (Mims and Mims, 2004). Dust from Lake Chad is rich in bacteria and fungi (Fa-
465 vet et al., 2013). These fungi would have also contributed to the elements detected in air



466 samplers. Bacteria are likely to accompany the dust particles, attached to their surface
467 (Yamaguchi et al., 2012; Prospero et al., 2005), but it is unknown whether any of these
468 organisms are still viable upon sedimentation across the central Amazon forest.

469 Up to half of all micronutrients in the canopy are stored in epiphytes (Cardelus
470 2010). Fungi housed within lichens take advantage of the large surface area provided by
471 their algal co-host, and are one of the most bio-absorbent organisms evolved for uptake
472 of minerals and other nutrients from atmospheric gases and particulates, and from both
473 dry deposition and rainfall. Another type of fungi common within the canopy are yeasts,
474 such as *Saccharomycetes* (Elbert et al., 2007; Womack et al., 2016).

475 During dry weather, as well as during fog and light rain events, dust deposits
476 onto the canopy and impacts directly onto leaves of vascular plants (e.g., trees and
477 vines), as well as epiphytic vascular and non-vascular plants, such as bryophytes (e.g.,
478 lichens, mosses and liverworts). Dust also settles onto ferns, and fungi within the cano-
479 py. Air samples from 40 m height showed fungi are common in the canopy. The small-
480 est and most metabolically active fungi detected in the canopy included lichens and
481 yeasts (Womack et al., 2015).

482 Up to 25,000 tons of phosphorus has been calculated as being deposited each
483 year on the Amazon. Meanwhile, a similar amount of phosphorus has been estimated to
484 be leached from rainforest soils (Yu et al., 2015). While much of the emphasis has been
485 on soil chemistry and root absorption, water-soluble minerals, as such as P and K, can
486 also be absorbed by leaves. Minerals, such as Fe, can be absorbed through plant leaves
487 as well (Fernandez and Brown, 2013). Thus, canopy deposition of Saharan dust is like-
488 ly to provide soluble iron to plants via their leaves, in addition to having an influence on
489 epiphytes and surface microorganisms.

490



491 **3.5 Iron availability**

492 The iron measurement results presented here show a predominance of Fe(III) in
493 the samples, while Fe(II), the form which plants can directly absorb, was measurable
494 only in four samples. The interest in determining the concentration of Fe(II) in aerosols,
495 besides being the ionic form absorbed by plants, is related to its much higher solubility
496 than Fe(III) (Zhu 1997). However, the efficiency in absorbing iron varies among species
497 and genotypes, although within plants the main form is Fe(III) (Kerbaui, 2012).

498 Therefore, plants develop specific strategies for Fe uptake (Hell and Stephan,
499 2003; Morrissey and Guerinot, 2009) and, added to this, abiotic factors such as pH, re-
500 dox state, and temperature can influence mineral nutrient speciation and solubility, as
501 can biotic factors. Plant roots also can modify the rhizosphere to affect nutrient availa-
502 bility; when challenged with a specific nutrient deficiency, plants can induce high-
503 affinity transporters and other mechanisms in their roots, to assist in meeting their min-
504 eral nutrient requirements (Grusak, 2001).

505 The pH of the environmental is important for solubility and therefore the availa-
506 bility of iron to microorganisms. More iron is present in solution in acid soils, but Fe is
507 less soluble in neutral or alkaline situations (Isaac, 1997). The majority of Amazon
508 Basin soils are acidic (Schmink and Wood, 1978) and, similar to Fe, Zn is also better
509 absorbed in soils with low pH (Broadley et al., 2007). In contrast, in alkaline soils, the
510 availability of Zn, Fe and Cu is very low (Marschner, 2012). However, the efficacy of
511 African dust as a fertilizer depends on many factors, such as particulate matter concen-
512 tration, composition, solubility, and bioavailability of element minerals. In addition,
513 fungi, the most common type of microorganism in the forest (Fracetto et al., 2013), can
514 readily absorb iron, in soluble and insoluble chemical states. Therefore, it is possible



515 that a small amount of atmospheric iron could affect the microbiota in the canopy, ra-
516 ther than have a significant effect on soil and root uptake for plants.

517 Iron availability in the canopy of forests has commonly been found to be limited
518 for growth of epiphytes, bacteria, and fungi (Crichton, 2009). Addition of iron can have
519 a variety of effects on plants and fungi, e.g., yeasts grown in iron-limiting culture show
520 a change in metabolism from fermentation to respiration upon the addition of iron
521 (Philpott et al., 2012). The ongoing deposition of micronutrients, such as iron, onto the
522 Amazon biota is likely to increase both epiphytic growth and fungal and bacterial de-
523 composition within the canopy. Previous observations described an increased tree fall
524 rate attributed to an abundance of epiphytes (Swap et al., 1992). Increase in iron bioa-
525 vailability is also known to increase the wood to root ratio, increase the rate of plant
526 growth, and increase nutrient cycling within a forest (Benzing, 1998; Crichton, 2009;
527 Cardelius, 2010). The full extent of the influence of Saharan dust is yet to be deter-
528 mined, although the majority of mineral nutrients available in the soil originate from the
529 gradual weathering of bedrock in the Amazon basin (Abouchami et al., 2013).

530

531 **4 Conclusion**

532 The current deposition of Saharan dust onto the Amazon is providing an iron-
533 rich source of essential macronutrients and micronutrients. The atmospheric deposition
534 of this nutrient-rich dust on the canopy is likely have an influence on rainforest ecology.
535 Previously unconsidered changes are likely occurring in growth patterns and decompo-
536 sition rates within the canopy, which affect carbon storage, release, and cycling in the
537 Amazon.

538 Overall, this study examined the bioavailability of soluble macro and micronu-
539 trients to plants of the Amazon Basin, and reported peaks in soluble Fe(III), Fe(II), Na,



540 Ca, K, and Mg during a major dust transport event from the Saharan desert, according
541 to meteorological (backward trajectories and wind field), remote sensing (aerosol opti-
542 cal depth), and *in situ* data analysis. In this way, the elemental contents of samples were
543 correlated with the arrival of African aerosols.

544 Our study also reported on the amount of soluble iron in two oxidation states,
545 Fe(II) and Fe(III), to understand how much of this element is bioavailable to the rain-
546 forest in the wet season.

547 Because these nutrients are added to the Amazon by atmospheric deposition they
548 will likely: 1) directly affect fungi within the canopy, as well as fungal-associated epi-
549 phytes, such as lichens. 2) have an influence on bacteria, and 3) provide nutrients direct-
550 ly to leaves and roots of other plants.

551

552 **Author contribution**

553 All authors contributed to the work presented in this paper. R.H.M. Godoi,
554 C.G.G. Barbosa, J.A. Rizzolo, A.F.F. Godoi, C. Pöhlker and A.O. Manzi developed the
555 concept, designed the study and the experiments and J. Rizzolo and I.H. Angelis carried
556 them out. C.I. Yamamoto, G. Borillo and A.O. Manzi provided reagents and gave ana-
557 lytical-technical support. C. Pöhlker, J. Saturno, D. Moran-Zuloagal and M.O. Sá col-
558 lected and analyzed data. R.H.M. Godoi, C.G.G. Barbosa, J.A. Rizzolo, P.E. Taylor,
559 L.V. Rizzo, N.E. Rosário, L.V. Rizzo, R.A.F. Souza, R.V. Andreoli, J. Saturno, D. Mo-
560 ran-Zuloaga and T. Pauliquevis analyzed data. C. Pöhlker, M.O. Andreae, F. Ditas, L.V.
561 Rizzo, E.G. Alves, T. Pauliquevis and P.E. Taylor gave conceptual advice. J.A. Rizzolo
562 prepared the manuscript and, with contributions from C.G.G. Barbosa, A.F.L. Godoi,
563 E.G. Alves, C. Pöhlker, C.I. Yamamoto, J. Saturno, D. Moran-Zuloaga, L.V. Rizzo,
564 N.E. Rosário, T. Pauliquevis, M.O. Andreae, P.E. Taylor and R.H.M. Godoi, discussed
565 the results and implications at all stages.

566

567

568

569



570 **Acknowledgments**

571 We acknowledge the support of the Fundação de Amparo à Pesquisa do Estado
572 do Amazonas (FAPEAM) and the Financiadora de Estudos e Projetos (FINEP). We
573 acknowledge logistical support from the Central Office of the Large Scale Biosphere
574 Atmosphere Experiment in Amazonia (LBA), the Instituto Nacional de Pesquisas da
575 Amazônia (INPA) and the Universidade do Estado do Amazonas (UEA). We also thank
576 the Max Planck Society and INPA for continuous support. We acknowledge the support
577 by the German Federal Ministry of Education and Research (BMBFcontract
578 01LB1001A) and the Brazilian Ministério da Ciência, Tecnologia e Inovação
579 (MCTI/FINEP contract 01.11.01248.00) as well as the UEA, FAPEAM, LBA/ INPA
580 and SDS/CEUC/RDS-Uatumã. We would like to especially thank all the people in-
581 volved in the logistical support of the ATTO project, in particular Reiner Ditz and Her-
582 mes Braga Xavier. We acknowledge the micrometeorological group of the INPA/LBA
583 for their collaboration concerning the meteorological parameters, with special thanks to
584 Marta Sa and Antonio Huxley. The authors would like to thank Dr. Jose Henrique Pe-
585 reira from Lawrence Berkeley National Laboratory for the enthusiastic and helpful sug-
586 gestions.

587

588

589

590 **References**

591 Abouchami, W., Nätke, K., Kumar, A., Galer, S. G., Jochum, K. P., Williams, E., Hor-
592 be, A. M. C., Rosa, J. W. C., Balsam, W., Adams, D., Mezgeri, K., and Andreae, M.
593 O.: Geochemical and isotopic characterization of the Bodélé Depression dust source



594 and implications for transatlantic dust transport to the Amazon Basin. *Earth and*
595 *Planetary Science Letters*, 380, 112-123, doi:10.1016/j.epsl.2013.08.028, 2013.

596

597 Andreae, M. O., Soot carbon and excess fine potassium: Long-range transport of com-
598 bustion-derived aerosols: *Science*, 220, 1148-1151, 1983.

599

600 Andreae, M. O., Acevedo, O. C., Araújo, A., Artaxo, P., Barbosa, C. G. G., Barbosa, H.
601 M. J., Brito, J., Carbone, S., Chi, X., Cintra, B. B. L., Silva, N. F., Dias, N. L., Dias-
602 Júnior, C. Q., Ditas, F., Ditz, R., Godoi, A. F. L., Godoi, R. H. M., Heimann, M.,
603 Hoffmann, T., Kesselmeier, J., Könemann, T., Krüger, M. L., Lavric, J. V., Manzi,
604 A. O., Lopes, A. P., Martins, D. L., Mikhailov, E. F., Moran-Zuloaga, D., Nelson, B.
605 W., Nölscher, A. C., Nogueira, D. S., Piedade, M. T. F., Pöhlker, C., Pöschl, U.,
606 Quesada, C. A., Rizzo, L. V., Ro, C.-U. Ruckteschler, N., Sá, L. D. A., Oliveira Sá,
607 M. C. B., Sales, R. M. N., Santos, J., Saturno, J., Schöngart, M., Sörgel, Souza, C.
608 M., Souza, R. A. F., Su, H., Targhetta, N., Tóta, J., Trebs, I., Trumbore, S., Eijck, A
609 van, Walter, D., Wang, Z., Weber, B., Williams, J., Winderlich, J., Wittmann, F.,
610 Wolff, S., and Yáñez-Serrano, A. M.: The Amazon Tall Tower Observatory (ATTO):
611 overview of pilot measurements on ecosystem ecology, meteorology, trace gases,
612 and aerosols. *Atmos. Chem. Phys.*, 15, 10723-10776, doi:10.5194/acp-15-10723-
613 2015, 2015.

614

615 Aragão, L. E. O. C.: The rainforest's water pump. *Nature*, 489, 7415, 217-218,
616 doi:10.1038/nature11485, 2012.

617



618 Arana, A., and Artaxo, P.: Composição elementar do aerossol atmosférico na região
619 central da Bacia Amazônica. *Química Nova*, 37(2), 268-276, 2014.

620

621 Artaxo, P., and Maenhaut, W.: Trace element concentrations and size distributions of
622 biogenic aerosols from the Amazon Basin during the wet season, *Nucl. Instrum.*
623 *Methods Phys. Res.*, 49, 366-371, doi:10.1016/0168-583X(90)90277-2, 1990.

624

625 Artaxo, P., Gerab, F., Yamasoe, M. A., and Martins, J. V.: Fine mode aerosol composi-
626 tion at three long-term atmospheric monitoring sites in the Amazon Basin: *J. Ge-*
627 *ophys. Res.*, 99, 22,857-22,868, doi:10.1029/94JD01023, 1994.

628

629 Artaxo, P., Martins, J. V., Yamasoe, M. A., Procópio, A. S., Pauliquevis, T. M., Andre-
630 ae, M. O., Guyon, P., Gatti, L. V., and Leal, A. M. C.: Physical and chemical proper-
631 ties of aerosols in the wet and dry seasons in Rondônia, Amazonia. *Journal of Geo-*
632 *physical Research*, 107(D20), 8081, doi:10.1029/2001JD000666, 2002.

633

634 Artaxo P., Rizzo, L. V., Brito, J. F., Barbosa, H. M. J., Arana A., Sena E. T., Cirino G.
635 G., Bastos W., Martins S. T., and Andreae M. O.: Atmospheric aerosol in Amazonia
636 and land use change: from natural biogenic to biomass burning conditions. *Faraday*
637 *Discuss.*, 165, 203-235, doi:10.1039/C3FD00052D, 2013.

638

639 Baars, H., Ansmann, A., Althausen, D., Engelmann, R., Artaxo, P., Pauliquevis T., and
640 Souza R.: Further evidence for significant smoke transport from Africa to Amazonia.
641 *Geophys. Res. Lett.*, 38, 1-6, doi:10.1029/2011GL049200, 2011.

642



- 643 Ben-Ami, Y., Koren I., Rudich Y., Artaxo P., Martin S T., and Andreae M. O.:
644 Transport of North African dust from the Bodélé depression to the Amazon Basin: a
645 case study. *Atmos. Chem. Phys.*, 10, 7533-7544, doi:10.5194/acp-10-7533-2010,
646 2010.
- 647
- 648 Benzing, D. H.: Vulnerabilities of tropical forests to climate change: the significance of
649 resident epiphytes. *Clim. Chang.* 39, 519-540, doi:10.1023/A:1005312307709, 1998.
- 650
- 651 BIPM. Evaluation of measurement data – Guide to the expression of uncertainty in
652 measurement JCGM 100:2008 (GUM 1995 with minor corrections), Paris: BIPM
653 Joint Committee for Guides in Metrology, 2008.
- 654 Bristow, C. S., Hudson-Edwards, K. A., and Chappell, A.: Fertilizing the Amazon and
655 equatorial Atlantic with West African dust. *Geophys. Res. Lett.*, 37, L14807,
656 doi:10.1029/2010GL043486, 2010.
- 657
- 658 Broadley, M. R, White, P. J, Hammond, J. P, Zelko, I., and Lux, A.: Zinc in plants. *New*
659 *Phytol.*, 173, 677-702, doi:10.1111/j.1469-8137.2007.01996.x, 2007.
- 660
- 661 Bruno, P., Caselli, M., Gennaro, G., Ielpo, P., and Traini, A.: Analysis of heavy metals
662 in atmospheric particulate by ion chromatography. *J. Chromatogr A.*, 888, 145-150,
663 doi:10.1016/S0021-9673(00)00503-3, 2000.
- 664
- 665 Cardelus, C. L.: Litter decomposition within the canopy and forest floor of three tree
666 species in a tropical lowland rain forest, Costa Rica. *Biotropica*, 42, 300-308,
667 doi:10.1111/j.1744-7429.2009.00590.x, 2010.



668

669 Creamean, J. M., Kaitlyn J., Suski, Rosenfeld, D., Cazorla, A., DeMott, P. J., Sullivan,
670 R. C., White, A. B., Ralph, F., M., Minnis, P., Comstock, J. M. Tomlinson, J. M.,
671 and Prather, K. A.: Dust and Biological Aerosols from the Sahara and Asia Influence
672 Precipitation in the Western U.S. *Science*, 339, 1572, doi:10.1126/science.1227279,
673 2013.

674

675 Crichton R. *Inorganic biochemistry of iron metabolism: from molecular mechanisms to*
676 *clinical consequences* 3rd Ed, Chichester: John Wiley and Sons, pp 461,
677 doi:10.1002/9780470010303, 2009.

678

679 Doughty, C. E., Metcalfe, D. B., Girardin, C. A. J., Amézquita, F. F., Cabrera, D. G.,
680 Huaraca Huasco, W., Silva-Espejo, J. E., Araujo-Murakami, A., Costa, M. C., Ro-
681 cha, W., Feldpausch, T. R., Mendoza, A. L. M., Costa, A. C. L., Meir, P., Phillips, O.
682 L., and Malhi, Y.: Drought impact on forest carbon dynamics and fluxes in Amazo-
683 nia. *Nature*. 519, 78-82, doi:10.1038/nature14213, 2015.

684

685 Draxler, R. R. and Rolph, G. D.: HYSPLIT (Hybrid Single-Particle Lagrangian Inte-
686 grated Trajectory) Model access via NOAA ARLREADY Website, available at:
687 <http://www.arl.noaa.gov/ready/hysplit4.html> (last access: 15 January 2016), NOAA
688 Air Resources Laboratory, Silver Spring, MD., 2015.

689

690 Elbert, W., Taylor, P. E., Andreae, M. O., and Pöschl, U.: Contribution of fungi to pri-
691 mary biogenic aerosols in the atmosphere: wet and dry discharged spores, carbohy-



692 drates, and inorganic ions. Atmos. Chem. Phys. 7, 4569-88, doi:10.5194/acp-7-4569,
693 2007.

694

695 Favet, J., Lapanje, A., Giongo, A., Kennedy, S., Aung, Y. Cattaneo, A., Davis-
696 Richardson, A. G., Brown, C. T. Kort, R., Brumsack, H., Schnetger, B., Chappell,
697 A., Kroijenga, J., Beck, A., Schwibbert, K., Mohamed, A. H., Kirchner, T., Dorr de
698 Quadros, P., Triplett, E. W., Broughton, W. J., and Gorbushina, A. A.: Microbial
699 hitchhikers on intercontinental dust: catching a lift in Chad. The ISME Journal, 7,
700 850-867, doi:10.1038/ismej.2012.152, 2013.

701

702 Fernandez V. and Brown P.: From plant surface to plant metabolism: the uncertain fate
703 of foliar applied nutrients. Front. Plant Sci., 4, 289, doi:10.3389/fpls.2013.00289,
704 2013.

705

706 Fracetto, G. M., Azevedo, L. C. B., Fracetto, F. J. C., Andreote, F. D., Lambais, M. R.,
707 and Pfenning, L. H.: Impact of Amazon land use on the community of soil fungi.
708 Sci. Agric. 70, 2, 59-67, doi:10.1590/S0103-90162013000200001, 2013.

709

710 Formenti, P., M. O. Andreae, L. Lange, G. Roberts, J. Cafmeyer, I. Rajta, W. Maenhaut,
711 B. N. Holben, P. Artaxo, and J. Lelieveld.: Saharan dust in Brazil and Suriname dur-
712 ing the Large-Scale Biosphere-Atmosphere Experiment in Amazonia (LBA)-
713 Cooperative LBA Regional Experiment (CLAIRE) in March 1998. J. Geophys. Res.,
714 106, 14919-14934, doi:10.1029/2000JD900827, 2001.

715



716 Garstang, M., Scala, J., Greco, S., Harris, R., Beck, S., Browell, E. Sacuse, G., Gregory,
717 G., Hill, G., Simpson, J., Tao, W., and Torre, A.: Trace gas exchange and convective
718 transports over the Amazonian rainforest. *J. Geophys. Res.*, 93, 1528-1550,
719 doi:10.1029/JD093iD02p01528, 1988.

720

721 Ginoux, P., Prospero, J. M., Gill, T. E., Hsu, N. C., and Zhao, M.: Global-scale attribu-
722 tion of anthropogenic and natural dust sources and their emission rates based on
723 MODIS Deep Blue aerosol products: *Rev. Geophys.*, 50, RG3005,
724 doi:10.1029/2012RG000388, 2012.

725

726 Goudie, A.S., and Middleton, N.J.: Saharan dust storms: nature and consequences.
727 *Earth-Sci. Rev.*, 56, 179-204, doi:10.1016/S0012-8252(01)00067-8, 2001.

728

729 Graham, B., Guyon, P., Taylor, P. E., Artaxo, P., Maenhaut, W., Glovsky, M. M., Flag-
730 an, R. C., and Andreae, M. O.: Organic compounds present in the natural Amazonian
731 aerosol: Characterization by gas chromatography-mass spectrometry. *J. Geophys.*
732 *Res.*, 108, 4766, doi:10.1029/2003JD003990, 2003.

733

734 Gross, A., Goren, T., Pio, C., Cardoso, J., Tirosh, O., Todd, M. C., Rosenfeld, D.,
735 Weiner, T., Custódio, D., and Angert, A.: Variability in Sources and Concentrations
736 of Saharan Dust Phosphorus over the Atlantic Ocean. *Environ. Sci. Technol. Lett.*,
737 2 (2), 31-37, doi:10.1021/ez500399z, 2015.

738

739 Gruzak, M. A.: Plant Macro- and Micronutrient Minerals. *Encyclopedia of Life Scienc-*
740 *es*. Nature Publishing Group, doi:10.1038/npg.els.0001306, 2001.



741

742 Guyon, P., Graham, B., Roberts, G. C., Mayol-Bracero, O. L., Maenhaut, W., Artaxo,
743 P., and Andreae, M. O.: Sources of optically active aerosol particles over the Ama-
744 zon forest. *Atmos. Environ.*, 38, 1039-1051, doi:10.1016/j.atmosenv.2003.10.051,
745 2004.

746

747 Haywood, J. M., Pelon, J., Formenti, P., Bharmal, N., Brooks, M., Capes, G., Chazette,
748 P., Chou, C., Christopher, S., Coe, H., and Cuesta, J. Overview of the dust and bio-
749 mass-burning experiment and African monsoon multidisciplinary analysis special
750 observing period-0. *Journal of Geophysical Research: Atmospheres*, 113(D23),
751 doi:10.1029/2008JD010077, 2008.

752

753 Hell, R., and Stephan U. W.: Iron uptake, trafficking and homeostasis in plants. *Planta*,
754 216, 541-551, doi:10.1007/s00425-002-0920-4, 2003.

755

756 Hochmuth, G.: Iron (Fe) nutrition in Plant U.S. Department of Agriculture, UF/IFAS
757 Extension Service, University of Florida, IFAS Document SL353, 2011.

758

759 Holben, B. N., Eck, T. F., Slutsker, I., Tanré, D., Buis, J. P., Setzer, A., Vermote, E.,
760 Reagan, J. A., Kaufman, Y. J., Nakajima, F., Lavenu, F., Jankowiak, I., and
761 Smirnov, A.: AERONET - A federated instrument network and data archive for aer-
762 osol characterization, *Rem. Sens. Environ.*, 66, 1-16, doi:10.1016/S0034-
763 4257(98)00031-5, 1998.

764

765 Hoornaert, S., Godoi, R. H. M., and Grieken, R. V.: Single particle characterization of



766 aerosol in the marine boundary layer and free troposphere over Tenerife, NE Atlan-
767 tic, during ACE-2. *J. Atmos. Chem.*, 46, 271-293, doi:10.1023/A:1026383403878,
768 2003.

769

770 Isaac, S.: Iron is relatively insoluble and often unavailable in the natural environment:
771 How do fungi obtain sufficient supplies? *Mycologist.*, 11, 41-42, 1997.

772

773 Karanasiou, A., Moreno, N., Moreno, T., Viana, M., Leeuw, F., and Querol, X.: Health
774 effects from Sahara dust episodes in Europe: Literature review and research gaps.
775 *Environ. Int.*, 47, 107-114, doi:10.1016/j.envint.2012.06.012, 2012.

776

777 Kerbauy, G. B. *Fisiologia Vegetal*. 2A edição, Rio de Janeiro: Guanabara Koogan, pp
778 431 2012.

779

780 Koren, I., Kaufman, Y. J., Washington, R., Todd, M. C., Rudich, Y., Martins, J. V., and
781 Rosenfeld, D.: The Bodélé depression: a single spot in the Sahara that provides most
782 of the mineral dust to the Amazon forest. *Environ. Res. Lett.*, 1, 1-5,
783 doi:10.1088/1748-9326/1/1/014005, 2006.

784

785 Mahowald, N. M., Engelstaedter, S., Luo, C., Sealy, A., Artaxo, P., Benitez-Nelson, C.,
786 Bonnet, S., Chen, Y., Chuang, P. Y., Cohen, D. D., Dulac, F., Herut, B., Johansen, A.
787 M., Kubilay, N., Losno, R., Maenhaut, W., Paytan, A., Prospero, J. M., Shank, L. M.,
788 and Siefert, R. L.: Atmospheric Iron Deposition: Global Distribution, Variability, and
789 Human Perturbations. *Annu. Rev. Mar. Sci.*, 1, 245-78,
790 doi:10.1146/annurev.marine.010908.163727, 2009.



791

792 Marschner, H.: Mineral nutrition of higher plants. Academic Press, London, pp 672,
793 2012.

794

795 Martin, S. T., Andreae M. O., Artaxo P., Baumgardner D., Chen Q., Goldstein A. H.,
796 Guenther, A., Heald C. L., Mayol-Bracero, O. L., McMurry, P. H., Pauliquevis, T.,
797 Pöschl, U., Prather, K. A., Roberts, G. C., Saleska, S. R., Silva Dias, M. A., Sprack-
798 len, D. V., Swietlicki, E., and Trebs I.: Sources and properties of Amazonian aerosol
799 particles. *Rev. Geophys.*, 48, RG2002, doi:10.1029/2008RG000280, 2010.

800

801 Mendez, J., Guieu, C., and Adkins, J.: Atmospheric input of manganese and iron to the
802 ocean: Seawater dissolution experiments with Saharan and North American dusts.
803 *Mar. Chem.*, 120, 34-43, doi:10.1016/j.marchem.2008.08.006, 2010.

804

805 Mims, S. A., and Mims, F. M.: Fungal spores are transported long distances in smoke
806 from biomass fires. *Atmos. Environ.*, 38, 5, 651-655,
807 doi:10.1016/j.atmosenv.2003.10.043, 2004.

808

809 Moosmüller, H., Chakrabarty, R. K., Ehlers, K. M., and Arnott, W. P.: Absorption Ång-
810 ström coefficient, brown carbon, and aerosols: basic concepts, bulk matter, and
811 spherical particles. *Atmospheric Chemistry and Physics*, 11(3), 1217-1225,
812 doi.org/10.5194/acp-11-1217-2011, 2011.

813

814 Morrissey, J. and Guerinot, M. L.: Iron uptake and transport in plants: The good, the
815 bad, and the ionome. *Chem. Rev.*, 109, 10, 4553-4567, doi:10.1021/cr900112r, 2009.



816

817 Okin, G. S., Mahowald, N., Chadwick, O. A., and Artaxo, P.: Impact of desert dust on
818 the biogeochemistry of phosphorus in terrestrial ecosystems, *Global Biogeochem.*
819 *Cycles*, 18, GB2005, doi:10.1029/2003GB002145, 2004.

820

821 Pauliquevis, T., Lara, L. L., Antunes, M. L., and Artaxo, P.: Aerosol and precipitation
822 chemistry measurements in a remote site in Central Amazonia: the role of biogenic
823 contribution. *Atmos. Chem. Phys.*, 12, 4987-5015, doi:10.5194/acp-12-4987, 2012.

824

825 Pérez-Sanz, A., and Lucena, J. J.: Synthetic iron oxides as sources of Fe in a hydropon-
826 ic culture of sunflower. In: ABADIA, J. *Iron nutrition in soils and plants*. Dordrecht:
827 Kluwer Academic, 241-246, doi:10.1007/978-94-011-0503-3_35, 1995.

828

829 Philpott, C.: Iron uptake in fungi: A system for every source. *BBA-Mol Cell Res.*, 1763,
830 7, 636-645, *Iron uptake in fungi: A system for every source*, 2006.

831

832 Philpott, C. C., Leidgens, S., and Frey, A. G.: Metabolic remodeling in iron-deficient
833 fungi. *Biochim Biophys Acta.*, 1823, 1509-1520, doi:10.1016/j.bbamcr.2012.01.012,
834 2012.

835

836 Prospero, J. M., Blades, E., Mathison, G., and Naidu, R.: Interhemispheric transport of
837 viable fungi and bacteria from Africa to the Caribbean with soil dust: *Aerobiologia*,
838 21, 1-19, doi:10.1007/s10453-004-5872-7, 2005.

839



840 Prospero, J. M., Collard, F. X., Molinie, J., and Jeannot, A.: Characterizing the annual
841 cycle of African dust transport to the Caribbean Basin and South America and its
842 impact on air quality and the environment. *Global Biogeochem. Cycles*, 29, 757-773,
843 doi:10.1002/2013GB004802, 2014.

844

845 Ravelo-Pérez, L. M., Rodríguez, S., Galindo, L., García, M. I., Alastuey, A., and López-
846 Solano, J.: Soluble iron dust export in the high altitude Saharan Air Layer. *Atmos.*
847 *Env.*, 133:49-59, doi:10.1016/j.atmosenv.2016.03.030, 2016.

848

849 Remer, L. A., Kaufman, Y. J., Tandr , D., Mattoo, S., Chu, D. A., Martins, J. V., Li, R-
850 R., Ichoku, C., Levy, R. C., Kleidman, R. G., Eck, T. F., Vermonte, E., and Holben,
851 B. N.: The MODIS Aerosol Algorithm, Products, and Validation Journal of the At-
852 mospheric Sciences. Special Section Volume, 62, 947-973, doi:10.1175/JAS3385.1,
853 2005.

854

855 Reynolds, R. L., Cattle, S. R., Moskowit, B. M., Goldstein, H. L., Yauk, K., Flagg, C.
856 B., Berqu , T. S., Kokaly, R. F., Morman, S., and Breit, G. N.: Iron oxide minerals in
857 dust of the Red Dawn event in eastern Australia, September 2009. *Aeolian Res.*, 15,
858 1-13, doi:10.1016/j.aeolia.2014.02.003, 2014.

859

860 Rienecker, M. R., Suarez, M. J., Gelaro, R., Todling, R., Bacmeister, J., Liu, E., Bosi-
861 lovich, M. G., Schubert, S. D., Takacs, L., Kim, G. K., Bloom, S., Chen, J., Collins,
862 D., Conaty, A., Silva, A. et al. MERRA: NASA's Modern-Era Retrospective Analy-
863 sis for Research and Applications. *J. Climate*, 24, 3624-3648, doi:10.1175/JCLI-D-
864 11-00015.1, 2011.



865

866 Rizzo, L. V., Artaxo, P., Müller, T., Wiedensohler, A., Paixão, M., Cirino, G. G., Arana,
867 A., Swietlicki, E., Roldin, P., Fors, E. O., Wiedemann, K. T., Leal, L. S. M., and
868 Kulmala, M.: Long term measurements of aerosol optical properties at a primary for-
869 est site in Amazonia. *Atmos. Chem. Phys.*, 13(17), 2391-2413, doi:10.5194/acp-13-
870 2391, 2013.

871

872 Salvador, P., Almeida, S. M., Cardoso, J., Almeida-Silva, M., Nunes, T., Cerqueira, M.,
873 Alves, C., Reis, M. A., Chaves, P. C., Artífano, B., and Pio, C.: Composition and
874 origin of PM₁₀ in Cape Verde: characterization of long-range transport episodes.
875 *Atmos. Environ.*, 127, 326-339, doi:10.1016/j.atmosenv.2015.12.057, 2016.

876

877 Schepanski, K., Tegen, I., and Macke, A.: Comparison of satellite based observations of
878 Saharan dust source areas. *Remote Sens. Environ.*, 123, 90-97,
879 doi:10.1016/j.rse.2012.03.019, 2012.

880

881 Schmink, M. and Wood, C.: *Frontier Expansion in Amazonia*, University of Florida
882 press, Gainseville, Florida, 1978.

883

884 Shi, Z., Bonneville, S., Krom, M. D., Carslaw, K. S., Jickells, T. D., Baker, A. R., and
885 Benning, L. G.: Iron dissolution kinetics of mineral dust at low pH during simulated
886 atmospheric processing. *Atmos. Chem. Phys.*, 11, 995-1007, doi:10.5194/acp-11-
887 995, 2011.

888



889 Siefert, R. L., Johansen A. M., and Hoffmann, M. R.: Measurements of trace metal (Fe,
890 Cu, Mn, Cr) oxidation states in fog and stratus clouds. *J. Air & Waste Manage. As-*
891 *soc.*, 48, 128-143, doi:10.1080/10473289.1998.10463659, 1998.

892

893 Swap, R., Garstang, M., Greco, S. Talbot, R., and Källberg, P.: Saharan dust in the Am-
894 azon Basin. *Tellus*, 44, 133-149, 1992.

895

896 Talbot, R. W., Andreae, M. O., Berresheim, H., Artaxo, P., Garstang, M., Harriss, R. C.,
897 Beecher, K. M., and Li, S. M.: Aerosol chemistry during the wet season in Central
898 Amazonia: The influence of long-range transport: *J. Geophys. Res.*, 95, 16,955-
899 16,969, 1990.

900

901 Trail, F., Xu, H., Loranger, R., and Gadoury, D.: Physiological and environmental as-
902 pects of ascospore discharge in *Gibberella zeae* (anamorph *Fusarium gramine-*
903 *arum*). *Mycologia*, 94, 181–189, 2002.

904

905 U.S. Environmental protection Agency. Test Methods for Evaluating Soil Waste, Physi-
906 cal/Chemical Methods, Method 3052: Microwave assisted acid digestion of siliceous
907 and organically based matrices. EPA SW-846, 1996.

908

909 U.S. Environmental protection Agency. Determination of inorganic anions in drinking
910 water by ion chromatography, Method 300.1. EPA, 1997.

911



912 Washington, R. and Todd, M. C.: Atmospheric controls on mineral dust emission from
913 the Bodélé Depression, Chad: The role of the low level jet, *Geophys. Res. Lett.*, 32,
914 L17701, doi:10.1029/2005GL023597, 2005.

915

916 Womack, A. M., Artaxo, P. E., Ishida, F. Y., Mueller, R. C., Saleska, S. R.,
917 Wiedemann, K. T., Bohannon, B. L. M., and Green, J. L.: Characterization of active
918 and total fungal communities in the atmosphere over the Amazon rainforest. *Biogeo-*
919 *sciences*, 12, 6337-6349, doi:10.5194/bg-12-6337, 2015.

920

921 Worobiec, A., Szalóki, I., Osán, J., Maenhaut, W., Stefaniak, E. A., and Grieken, R. V.
922 Characterization of Amazon Basin aerosols at the individual particle level by X-ray
923 microanalytical techniques.: *Atmos. Environ.*, 41, 9217-9230,
924 doi:10.1016/j.atmosenv.2007.07.056, 2007.

925

926 Yamaguchi, N., Ichijo, T., Sakotani, A., Baba, T., and Nasu, M.: Global dispersion of
927 bacterial cells on Asian dust. *Sci Rep.* 2, 525, doi:10.1038/srep00525, 2012.

928

929 Yu, H., Chin, M., Yuan, T., Bian, H., Remer, L. A., Prospero, J. M., Omar, A., Winker,
930 D., Yang, Y., Zhang, Y., Zhang, Z., and Zhao, C.: The fertilizing role of African dust
931 in the Amazon rainforest: A first multiyear assessment based on data from Cloud-
932 Aerosol Lidar and Infrared Pathfinder Satellite Observations. *Geophys. Res. Lett.*,
933 42, 1984-1991, doi:10.1002/2015GL063040, 2015.

934

935 Zhang, Z., Engling, G., Zhang, L., Kawamura, K., Yang, Y., Tao, J., Zhang, R., Chan,
936 C., and Li, Y.: Significant influence of fungi on coarse carbonaceous and potassium



937 aerosols in a tropical rainforest. Environ. Res. Lett., 10, 034015, doi:10.1088/1748-

938 9326/10/3/034015, 2015.

939

940 Zhu, X. R., Prospero, J. M., and Millero, F. J.: Diel variability of soluble Fe(II) and sol-

941 uble total Fe in North African dust in the trade winds at Barbados. J. Geophys. Res.,

942 102, 21297-21305, doi:10.1029/97JD01313 , 1997.

943

944